Location Selection of Fast-Charging Station for Heavy-Duty EVs Using GIS and Grid Analysis

Preprint

Mingzhi Zhang, Xiangqi Zhu, Barry Mather, Pranav Kulkarni, and Andrew Meintz

National Renewable Energy Laboratory

Presented at the 2021 IEEE Innovative Smart Grid Technologies, North America (ISGT NA)
February 15–18, 2021

NREL is a national laboratory of the U.S. Department of Energy
Office of Energy Efficiency & Renewable Energy
Operated by the Alliance for Sustainable Energy, LLC

This report is available at no cost from the National Renewable Energy Laboratory (NREL) at www.nrel.gov/publications.

Contract No. DE-AC36-08GO28308

Conference Paper
NREL/CP-5D00-77823
February 2021

Location Selection of Fast-Charging Station for Heavy-Duty EVs Using GIS and Grid Analysis

Preprint

Mingzhi Zhang, Xiangqi Zhu, Barry Mather,
Pranav Kulkarni, and Andrew Meintz

National Renewable Energy Laboratory

Suggested Citation
Zhang, Mingzhi, Xiangqi Zhu, Barry Mather, Pranav Kulkarni, and Andrew Meintz. 2021. *Location Selection of Fast-Charging Station for Heavy-Duty EVs Using GIS and Grid Analysis: Preprint*. Golden, CO: National Renewable Energy Laboratory. NREL/CP-5D00-77823. https://www.nrel.gov/docs/fy21osti/77823.pdf.

NREL is a national laboratory of the U.S. Department of Energy
Office of Energy Efficiency & Renewable Energy
Operated by the Alliance for Sustainable Energy, LLC

This report is available at no cost from the National Renewable Energy Laboratory (NREL) at www.nrel.gov/publications.

Contract No. DE-AC36-08GO28308

Conference Paper
NREL/CP-5D00-77823
February 2021

National Renewable Energy Laboratory
15013 Denver West Parkway
Golden, CO 80401
303-275-3000 • www.nrel.gov

NOTICE

This work was authored in part by the National Renewable Energy Laboratory, operated by Alliance for Sustainable Energy, LLC, for the U.S. Department of Energy (DOE) under Contract No. DE-AC36-08GO28308. Funding provided by the U.S. Department of Energy Office of Energy Efficiency and Renewable Energy Vehicle Technologies Office via the 1+MW Medium Duty/Heavy Duty Vehicle Project. The views expressed herein do not necessarily represent the views of the DOE or the U.S. Government.

Location Selection of Fast-Charging Station for Heavy-Duty EVs Using GIS and Grid Analysis

Mingzhi Zhang, Xiangqi Zhu,
Barry Mather and Pranav Kulkarni
Power Systems Engineering Center
National Renewable Energy Laboratory
Golden, CO, USA
mingzhi.zhang@nrel.gov, xiangqi.zhu@nrel.gov,
barry.mather@nrel.gov, pranav.kulkarni@nrel.gov

Andrew Meintz
Center for Integrated Mobility Sciences
National Renewable Energy Laboratory
Golden, CO, USA
andrew.meintz@nrel.gov

***Abstract*—This work presents a systematic methodology for the location selection of fast-charging stations for heavy-duty electric vehicles (EVs) based on both geospatial and electric grid analysis. The geospatial analysis is based on real-world geographic information system (GIS) data of road networks and existing supportive infrastructures. The grid analysis is implemented based on node-level analysis of potential impacts on voltages and power losses in the distribution system. A case study using a realistic, three-phase, unbalanced distribution feeder from California and extracted real-world GIS data is used to demonstrate the intuitiveness and effectiveness of the proposed methodology for the location selection of fast-charging stations for heavy-duty EVs considering both electric and existing transportation infrastructures.**

Keywords—Heavy-duty EVs, fast-charging stations, location selection, grid analysis, GIS, transportation.

I. Introduction

According to data from the Bureau of Transportation Statistics [1], the relative share of truck-based commercial freight is nearly 70% by mode of transportation, and it is estimated that 15.5 million trucks—mostly conventional heavy-duty diesel trucks—are operating in the United States. In the past, heavy-duty electric vehicles (EVs) have not been a viable option because of the high energy requirements and low energy density of batteries, but because of recent developments in battery technology and the continuous decrease in battery costs, it is estimated that the life-cycle costs of heavy-duty electric trucks may already be less than those of heavy-duty diesel trucks, making the electrification technically and commercially feasible [2]. The lack of en route fast charging facilities for long distance travel, however, is another limitation of truck electrification. To fill this need, public charging stations are expected to emerge on high-density freight corridors to provide charging services to heavy-duty EVs.

For the placement and sizing of charging stations for a region, a graph-based approach was proposed in [3]. The objective is to limit the waiting time for all charging stations in the road network below a reasonable threshold; however, this approach works only for large regional scale planning like state level and does not consider the impacts of charging stations on the power system network. The same issues exist in [4], which used a transportation-oriented optimization approach to allocate charging stations along highway corridors. The integration of EVs could bring challenges to power systems, such as increased peak load [5], power quality issues [6], [7], increased power losses, and shortened life of transformers [8]. Considering the nature of charging infrastructure, understanding grid impacts should be an important factor when planning fast-charging stations for heavy-duty EVs.

Coordinated transportation and electric power network planning were discussed in [9] by formulating a nonlinear, optimization-based planning problem. Similarly, a multi-objective, optimization-based planning model was proposed in [10] for fast-charging EV stations. The proposed transportation planning model is based on the assumption that the traffic patterns of EVs are known, but that access to real-world travel data to support the assumed spatial-temporal distribution of EV transportation behaviors is difficult to obtain. How to accurately and realistically model and analyze the coupling between the transportation and power system and then effectively select the appropriate locations for EV charging stations are involved processes requiring significant data resources and is still an open research topic.

In this paper, we focus on the location selection of fast-charging stations for heavy-duty EVs. From the perspective of electric grid operation, we provide a ranking method based on the charging station's potential impacts on system voltage and power losses to compare candidate charging station locations. Meanwhile, real-world geographic information system (GIS) data—including road networks and existing supportive infrastructures—are extracted for the utility service region to provide support for the fast-charging station location selection from the perspective of geospatial analysis.

This paper is organized as follows: Section II introduces the proposed methodology for the selection of fast-charging stations heavy-duty EVs. Section III presents how the proposed methodology works on a realistic feeder from California with extracted real-world GIS data. Section IV concludes the paper and presents potential future work.

II. Analysis Methodology

In this section, we first introduce the methods for extracting real-world GIS data for geospatial analysis. Then we present grid impact analysis that provides a ranking method for all electric nodes by evaluating the EV charging station's potential impacts on distribution system voltages and losses.

A. GIS-Based Geospatial Analysis for Location Selection

The geospatial-based analysis is based on real-world GIS data, which are extracted from OpenStreetMap (OSM). OSM is a global collaborative (crowd-sourced) data set that aims to create a free editable map of the world. An open-source package, OSMnx [11], is used to retrieve, analyze, and visualize street networks from OSM through the Overpass application programming interface and to retrieve data about existing infrastructure, such as restaurants, gas stations, and many different kinds of buildings. GeoPandas [12] is used in the analysis process to manipulate and study the extracted geospatial data. The extracted road network is saved as a directed graph, which can also be used in other transportation-related applications, such as EV charging navigation.

To define fast-charging stations for heavy-duty EVs on high-density freight corridors, in this work, the location selection first considers how to minimize the deviations from drivers' desired trip paths; therefore, the charging station should be located in the areas near highway corridors. Existing infrastructure that have supportive functions for heavy-duty EV drivers, such as food services, are considered to be more feasible and desirable charging station locations [13]. A heuristic-based score system is designed to quantitatively compare the feasibility of different highway exits for charging station placement based on the number of supportive infrastructures in adjacent areas. An example of the score system is demonstrated in the Section III case study. The supportive infrastructure list can be adjusted if real survey data from heavy-duty EV truck drivers can be obtained. Using this presented GIS data extraction method, other factors associated with existing transportation infrastructure and auxiliary facilities can also be added, if needed.

B. Grid Impact Analysis for Location Selection

Two types of major impacts on the distribution system brought by EV charging load integration are large voltage deviations and increased system losses; therefore, the relationship between node power injections and node voltage /system loss variations can be used to evaluate the grid impacts of different EV charging station locations. A generic, three-phase, unbalanced formulation with feeder-head substation chosen as the slack bus is used to model the distribution system. The active/reactive power injections of Y/Δ-connected distributed energy resources or loads on each bus can be defined as: $P^Y = \Re(s^Y)$, $Q^Y = \Im(s^Y)$, $P^\Delta = \Re(s^\Delta)$, and $Q^\Delta = \Im(s^\Delta)$. The real and reactive power injection vectors for the distribution system are defined as $\mathbf{x}^Y = [(\mathbf{p}^\mathrm{Y})^\top, (\mathbf{q}^\mathrm{Y})^\top]^\top$, $\mathbf{x}^\Delta$=$[(\mathbf{p}^\Delta)^\top$, and $(\mathbf{q}^\Delta)^\top]^\top$.

1) Voltage load sensitivity matrix

A fixed-point-based power flow linearization method [14] is used to achieve the approximated linear relations between the node power injections and voltages, which can be defined as:

$$\begin{aligned} \tilde{\mathbf{v}} = &\quad \mathbf{M}_{\tilde{\mathbf{v}}}^{\mathrm{Y}}\mathbf{x}^{\mathrm{Y}} + \mathbf{M}_{\tilde{\mathbf{v}}}^{\Delta}\mathbf{x}^{\Delta} + \boldsymbol{\alpha} \\ |\tilde{\mathbf{v}}| = &\quad \mathbf{S}_{|\mathbf{v}|}^{\mathrm{Y}}\mathbf{x}^{\mathrm{Y}} + \mathbf{S}_{|\mathbf{v}|}^{\Delta}\mathbf{x}^{\Delta} + \boldsymbol{\beta} \end{aligned} \tag{1}$$

For a given set of power injections, $\mathbf{x}^Y, \mathbf{x}^\Delta$, the first iteration of the fixed-point method provides the explicit and complex value versions of the voltage sensitivities to both the Y and Δ power injections:

$$\begin{aligned} \mathbf{M}_{\tilde{\mathbf{v}}}^{\mathrm{Y}} = &\quad \left[\mathbf{Y}_{LL}^{-1}diag(\overline{\hat{\mathbf{v}}})^{-1}, -j\mathbf{Y}_{LL}^{-1}diag(\overline{\hat{\mathbf{v}}})^{-1}\right] \\ \mathbf{M}_{\tilde{\mathbf{v}}}^{\Delta} = &\quad \left[\mathbf{Y}_{LL}^{-1}\mathbf{H}^\top diag(\mathbf{H}\overline{\hat{\mathbf{v}}})^{-1}, -j\mathbf{Y}_{LL}^{-1}\mathbf{H}^\top diag(\mathbf{H}\hat{\mathbf{v}})^{-1}\right] \end{aligned} \tag{2}$$

where both $\mathbf{M}_{\tilde{\mathbf{v}}}^{\mathrm{Y}}$ and $\mathbf{M}_{\tilde{\mathbf{v}}}^{\Delta}$ are in the dimension of $\mathbb{D}^{3N\times 6N}$, N is the system bus number, and α in (1) equals no-load voltage $\mathbf{w} = \mathbf{Y}_{LL}^{-1}\mathbf{Y}_{L0}\mathbf{v}^0$.

According to the mathematical rule of deviation:

$$\frac{\partial|f(x)|}{\partial x} = \frac{1}{|f(x)|}\Re\left[\overline{f(x)}\frac{\partial f(x)}{\partial x}\right] \tag{3}$$

The sensitivities of the node voltage magnitude, $|\mathbf{v}|$, to power injections $\mathbf{x}^\mathrm{Y}$, $\mathbf{x}^\Delta$ can be derived from (2) as:

$$\begin{aligned} \mathbf{S}_{|\mathbf{v}|}^{\mathrm{Y}} = \frac{\partial|\mathbf{v}|}{\partial\mathbf{x}^{\mathrm{Y}}} &= diag(|\hat{\mathbf{v}}|)^{-1}\Re\left[diag(\hat{\mathbf{v}})\mathbf{M}_{\tilde{\mathbf{v}}}^{\mathrm{Y}}\right] \\ \mathbf{S}_{|\mathbf{v}|}^{\Delta} = \frac{\partial|\mathbf{v}|}{\partial\mathbf{x}^{\Delta}} &= diag(|\hat{\mathbf{v}}|)^{-1}\Re\left[diag(\hat{\mathbf{v}})\mathbf{M}_{\tilde{\mathbf{v}}}^{\Delta}\right] \\ \boldsymbol{\beta} &= |\hat{\mathbf{v}}| - \mathbf{M}_{|\mathbf{v}|}^{\mathrm{Y}}\hat{\mathbf{x}}^{\mathrm{Y}} - \mathbf{M}_{|\mathbf{v}|}^{\Delta}\hat{\mathbf{x}}^{\Delta} \end{aligned} \tag{4}$$

This linear approximation is different from local approximation approaches, such as the first-order Taylor method. An interpolation between specific loading condition and the no-load condition is derived for the approximation; this can achieve a better global behavior approximation and therefore perform better under scenarios of high penetrations of renewable generation. A more detailed analysis of the upper bound of the approximation error and its computation efficiency can be found in [14].

2) Loss load sensitivity matrix

In addition to the impacts on voltages, the placement of fast-charging stations in the existing distribution system could increase system power losses. Power losses in the distribution system are caused mainly by currents flowing over the distribution power lines, which are closely related to the reactance of power flow paths between the feeder head and load nodes; therefore, indicators are needed to show the relationship between the nodal real/reactive power injections and the system losses. A perturbation-based method is proposed to achieve the approximated relationship between node power variations and system power losses, which are defined as:

$$\mathbf{L_P} = \mathbf{L_P^Y}\mathbf{x}^{\mathrm{Y}} + \mathbf{L_P^\Delta}\mathbf{x}^{\Delta} + \boldsymbol{\gamma} \tag{5}$$

where $\mathbf{L}_\mathrm{P}^{(\mathrm{Y}/\Delta)}$ is in dimension of $\mathbb{D}^{3N\times 1}$, which is defined as a loss-of-load sensitivity matrix (LLSM). The elements in the LLSM stand for the approximated relationship between the node-level power variations and the system active power losses. For the node that has a high value of loss-of-load sensitivity, higher power losses will result from the integration of EV charging loads than for nodes with lower values. The procedures for the perturbation-based LLSM calculation are shown in Algorithm 1.

Algorithm 1: Perturbation-based LLSM calculation

Step 1: Construct power perturbation vector for node i, $\Delta S_i = \Delta P_i + \Delta Q_i$, then update $\mathbf{x}^\mathrm{Y}, \mathbf{x}^\Delta$
Step 2: Update system voltage vector using derived voltage sensitivities matrix, $\tilde{\mathbf{v}} = \mathbf{M}_{\tilde{\mathbf{v}}}^{\mathrm{Y}}\mathbf{x}^{\mathrm{Y}} + \mathbf{M}_{\tilde{\mathbf{v}}}^{\Delta}\mathbf{x}^{\Delta} + \boldsymbol{\alpha}$
Step 3: Calculate new system losses using system admittance matrix and updated voltage vector, $L = \tilde{\mathbf{v}}\bar{Y}\bar{\mathbf{v}}$
Step 4: Calculate power loss variation ΔL and then the losses sensitivity $\mathbf{L}_\mathrm{P}^{(\mathrm{Y}/\Delta)}$ for node i, $\Delta L/\Delta S_i$
Step 5: Repeat steps 1–4 for all other nodes, and obtain the system loss load sensitivity matrix, $\mathbf{L}_\mathrm{P}$, for all nodes

3) Electric impact score

The derived voltage and LLSM can be used to compare the grid impact of integrating different EV charging station locations. For voltage magnitude sensitivities $\mathbf{S}_{|\mathbf{v}|}^{\mathrm{Y}}, \mathbf{S}_{|\mathbf{v}|}^{\Delta}$ in (4), because different voltage levels could exist in the system, to achieve meaningful comparisons among different nodes, they are converted to per-unit, value-based voltage sensitivities

$\mathbf{S}_{\mathbf{vpu}}^{\mathrm{Y}}, \mathbf{S}_{\mathbf{vpu}}^{\Delta}$. Both $\mathbf{S}_{\mathbf{vpu}}^{\mathrm{Y}}$ and $\mathbf{S}_{\mathbf{vpu}}^{\Delta}$ are in complex form; and the real and imaginary parts can be defined as $VLSM_P$ and $VLSM_Q$, respectively, in dimension of $\mathbb{D}^{3N\times 3N}$. The node voltage deviations caused by node power variations can be expressed as:

$$\delta V_{pu} = VLSM_P \delta P + VLSM_Q \delta Q \tag{6}$$

$$\begin{bmatrix} \delta V_1 \\ \vdots \\ \delta V_n \end{bmatrix} = \begin{bmatrix} p_{11} & \cdots & p_{1n} \\ \vdots & \ddots & \vdots \\ p_{n1} & \cdots & p_{nn} \end{bmatrix} \begin{bmatrix} \delta P_1 \\ \vdots \\ \delta P_n \end{bmatrix} + \begin{bmatrix} q_{11} & \cdots & q_{1n} \\ \vdots & \ddots & \vdots \\ q_{n1} & \cdots & q_{nn} \end{bmatrix} \begin{bmatrix} \delta Q_1 \\ \vdots \\ \delta Q_n \end{bmatrix} \tag{7}$$

p_{ij} and q_{ij} are elements in $VLSM_P$ and $VLSM_Q$, which represent the voltage deviations on node i for a unit deviation of real/reactive power injection on node j, respectively. The voltage deviations on all nodes if a power disturbance $[\delta P_j, \delta Q_j]$ is put on node j can be derived as：

$$\begin{bmatrix} \delta V_1 \\ \vdots \\ \delta V_n \end{bmatrix} = \begin{bmatrix} p_{1j} \\ \vdots \\ p_{nj} \end{bmatrix} [\delta P_j] + \begin{bmatrix} q_{1j} \\ \vdots \\ q_{nj} \end{bmatrix} [\delta Q_j] \tag{8}$$

Therefore, the voltage impact factor, $\mathrm{I}_{(\mathrm{V},\, \mathrm{j})}$, for node j can be defined as the summation of the absolute values of the elements in column j of $VLSM_P$ and $VLSM_Q$ as:

$$\mathrm{I}_{(\mathrm{V},\, \mathrm{j})} = \sum_{i=1}^{n} \left| p_{ij} + q_{ij} \tan\theta_j \right| \tag{9}$$

where θ_j is the phase angle of load on node j. Note that this impact factor formulation can integrate the reactive power support capability of inverters into the potential impact evaluation process.

The min-max feature scaling is then used to map all node impact values, $\mathrm{I}_{(\mathrm{V},\, \mathrm{j})}$, into the range from [0,1] and saved into a vector of voltage impact score, $\boldsymbol{I_V}$. A higher normalized voltage impact factor in $\boldsymbol{I_V}$ means larger potential disturbances on system voltages. Similarly, the loss sensitivities, $\mathbf{L}_{\mathrm{P}}$, are also normalized into the range from [0,1] as a loss impact score, $\boldsymbol{I_L}$. For the node that has a high value of loss sensitivities, a higher impact score will be assigned to it in the fast-charging station location selection process to reduce the potential system power losses introduced by the integration of EV charging loads. Then a ranking method is designed to provide a comparison index for all electric nodes from the perspective of grid impact analysis. The electric impact score for each node can be defined as:

$$\boldsymbol{I_{grid}} = \alpha \boldsymbol{I_V} + \beta \boldsymbol{I_L} \tag{10}$$

where α, β are coefficients for the voltage impact score and system power loss score, which can be designated according to the system characteristics and operation preferences.

III. Case Study

This section presents a case study of charging station location selection on a realistic California feeder. First, we perform geospatial analysis using the real-world GIS data of road networks and existing supportive infrastructure for the target area. Then we perform the electric system analysis to provide impact scores for all the nodes to compare their potential impacts on a distribution system. Finally, we discuss a comprehensive analysis of EV charging station location selection based on both geospatial and electric grid analysis. To protect the sensitive information of the utility feeder, we select an area that has a similar shape to the realistic feeder area, which can be used to demonstrate the proposed charging station location selection method without revealing the real location of the feeder.

A. Transportation Analysis

The road network and existing infrastructure GIS data for the area of interest are extracted using the proposed methodology in Section II.A. The road networks are modeled and visualized as a directed graph, as shown in Fig. 1.

Fig. 1. Road network for the research target area

According to the road network analysis, we locate four highway exits: A, B, C, and D. To minimize deviation from drivers' desired trip paths, the areas near the highway exits are chosen as potential locations for fast-charging stations for heavy duty EVs. In addition, GIS data from all existing infrastructure near the highway exits are extracted and visualized as a point or a polygon according to their geospatial shapes and sizes, as shown in Fig. 2. Roads are visualized as black graphs, and infrastructure are visualized as blue polygons.

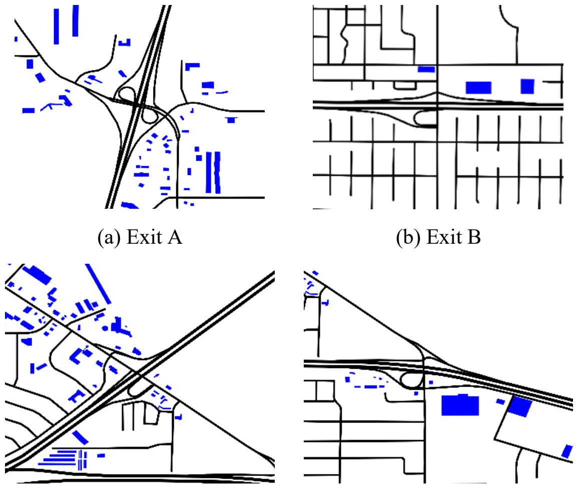

(a) Exit A (b) Exit B

(c) Exit C (d) Exit D

Fig. 2. Highway exits and existing infrastructure

The supportive infrastructure near the four exits are also considered in the EV charging station location selection process—for example, existing parking lots could be upgraded to provide charging services to EVs. A score reference for all types of supportive infrastructure considered in the case study is listed in Table 1. The weights and categories of different types of supportive infrastructure can be adjusted based on survey results from the drivers of heavy-duty electric trucks about their habits and preference.

TABLE I. Score Design for Attraction Infrastructure

Attraction Infrastructures	Food Services	Gas Station/ Rest Center	Parking Lots
Score	1	3	2

According to the GIS data analysis, there is little supportive infrastructure near highway exit B, so we do not consider it in the charging station selection process. According to the geospatial scale analysis, for example, there exists 10 food service merchants, 3 fuel stations, and 3 parking lots that are large enough to be able to accommodate heavy-duty EVs near Exit A, so the total score for Exit A from the perspective of transportation analysis is 25. The number of supportive infrastructure in the area near exits A, C, and D and the total transportation scores are listed in Table 2.

TABLE II. ATTRACTION INFRASTRUCTURES SUMMARY

Highway Exit	Food Services	Gas Station	Parking Lots	Total Score
A	10	3	3	25
C	16	6	9	52
D	8	2	5	24

B. Electric System Analysis

A realistic feeder is used to demonstrate the proposed methods for location selection based on grid impacts analysis. The feeder has a length of 13.7 mi. (22 km), and the peak system active and reactive power load is 3.069 MW and 1.302 MVAR, respectively. The proposed grid impact analysis is based on the derived voltage and loss-of-load sensitivities. The accuracy of the proposed sensitivity calculation method is validated by comparing it with the power flow results from OpenDSS. Because of the lack of time-series load profiles for the test feeder, a random load profile generation method is proposed to simulate all possible load combination scenarios for the test feeder. All the loads in the test feeder are modeled as a constant power load in the validation process. For each load in the test feeder, a uniformly distributed random number between 0 and 1.5 is multiplied to its nominal power value to model the load variations. Then the new system voltages and losses are calculated using both the proposed linearized power flow model and OpenDSS under this new load scenario. For each scenario, the maximum node voltage deviation ratio is defined as in (11) to achieve the node level voltage comparison:

$$max\left|\frac{V_{linearized}-V_{OpenDSS}}{V_{OpenDSS}}\right| \tag{11}$$

The comparison is repeated 10,000 times under all kinds of different system load scenarios to show the performance of the proposed linearization model. The distribution of the maximum node-level voltage magnitude deviations for all 10,000 scenarios is shown in Fig. 3. Similarly, the distribution of the power loss deviations is shown in Fig. 4. The maximum node-level voltage magnitude and system power loss deviations are near 0.45% and 1% respectively, which shows that the proposed sensitivity calculation method can achieve high accuracy under all load conditions.

Based on the electric impact score defined in (10), and assuming that the coefficients for the voltage disturbance impacts and system power loss impacts are the same, the higher the impact score is, the higher the potential grid impact if this node is selected as the location for the fast-charging station; therefore, different nodes in a test feeder as candidates for EV charging stations can be easily compared using the proposed electric impact scores, and the scores provide a comparative index for the charging station location selection from the perspective of power system analysis. Fig. 5 shows the ranking results for the feeder nodes according to the calculated grid impact scores, nodes near Exit A and C are framed by black boxes. The specific coordinates and electrical connections of different buses are not shown in the figure due to the sensitive information involved, but the markers in the picture represent the relative geographic locations of different buses in the feeder. It should be noted that the electrical impact score is not dependent on geographic location, but rather on the electrical connection method and grid line parameters. Therefore, it is possible to have large differences in impact scores in the same region and this phenomenon illustrates the value of the proposed method in providing comparison criteria for different nodes in same area. There technically exists several best/good locations in the general worst areas, but these places are not good candidates for placing charging stations because they are sparsely distributed in that area and not be able to connect a big charging station physically. Therefore, the general best/good areas are recommended for real world charging station placement.

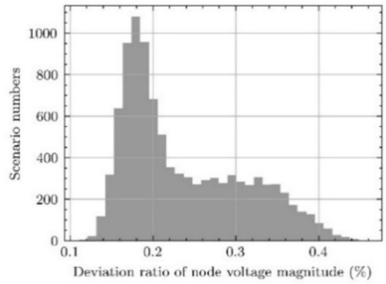

Fig. 3. Distribution of maximum node voltage and loss deviation ratio

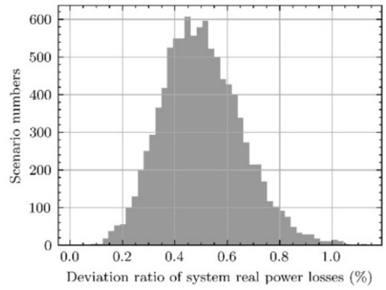

Fig. 4. Distribution of maximum loss deviation ratio

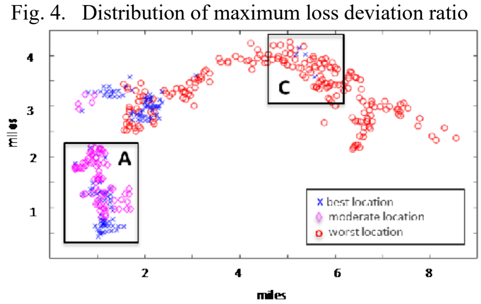

Fig. 5. Candidate location comparisons on a test feeder

C. Comprehensive Analysis for EV Charging Station Location Selection

The areas near the highway exits are marked on the electric grid network in Fig. 6 to show the coupling effects of the road network and the electric grid network. Based on the transportation analysis, the area near Exit B is excluded because it lacks supportive infrastructure, and the areas near Exit C and Exit D have higher scores than Exit A. But the impact scores of the location candidates in the area near Exit D are much higher than near Exit A, which is because the area near Exit D is near the end of the distribution feeder. Integrating new EV charging loads in this area will cause a considerable system voltage drop and increased power losses, so electric nodes near Exit D are excluded as candidates for fast-charging stations.

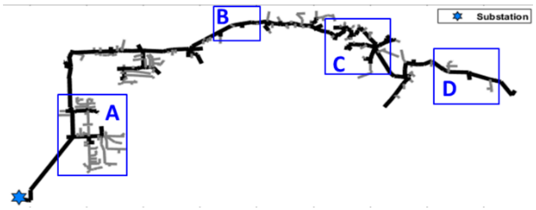

Fig. 6. Coupling of the road network and electric grid network

The charging station plays the role of a major connection point between the transportation and electric power infrastructures. The influential factors in both the transportation and electric areas need to be considered and balanced in the planning process. The locations and geographic shapes of all existing supportive infrastructure near Exit A and Exit C with the extracted road network are shown in Fig. 7. The fuel stations are marked as red circles, the food service sites are marked as green circles, and the parking lots are marked in blue according to the geographic shapes. All of this infrastructure already has access to the local electric grid, so selecting this infrastructure as candidates for fast-charging stations can usually save construction and installment costs.

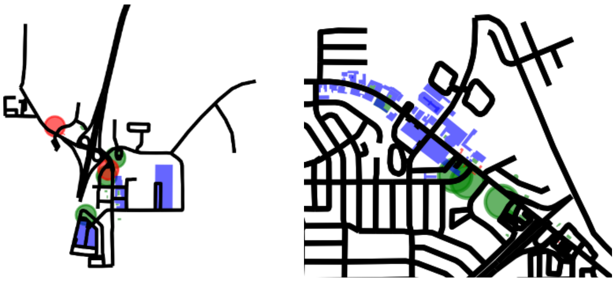

Fig. 7. Road network and supportive infrastructure near Exit A and Exit C

Location candidates near Exit C have a higher preference for fast-charging stations from the perspective of transportation analysis, but they also have a higher average for potential impacts than candidates near Exit A; therefore, the electric impact score calculated by (10) together with the transportation travel amenities analysis score shown in Table II can be used to compare and select the best electric node as the EV charging station location. Different weights can be put on the transportation analysis score and electric impact score to emphasize preferred charging station placement considerations. For example, if we put a higher weight on the electric impact score, a connection point from area A would be better; but if we put a higher weight on the transportation analysis score, locations in area C would satisfy our needs.

IV. Conclusions and Future Work

This paper presented a systematic methodology for the location selection of fast-charging EV stations based on transportation and electric grid analysis. A realistic, unbalanced distribution feeder and the coupled, real-world transportation network were used to demonstrate the influential factors that must be considered and well balanced in the location selection planning process. The proposed transportation analysis and electric impact scores can provide quantitative comparison indexes for potential location candidates of fast-charging stations to serve heavy-duty EVs.. This methodology can also be extended for light duty charging stations, with some modifications on the factors to be considered. Potential future work includes an EV charging guidance design that combines extracted road network GIS data, real-world vehicle travel patterns, network effects of the chosen locations, real-time traffic conditions, detailed existing infrastructure and services for heavy-duty trucks, and an optimal operation control strategy for EV charging stations that considers both the energy price and operating conditions.

Acknowledgments

Map data copyrighted by OpenStreetMap contributors and available from https://www.openstreetmap.org. This work was authored by the National Renewable Energy Laboratory, operated by Alliance for Sustainable Energy, LLC, for the U.S. Department of Energy (DOE) under Contract No. DE-AC36-08GO28308. Funding provided by U.S. Department of Energy Office of Energy Efficiency and Renewable Energy Vehicle Technologies Office via the 1+MW Medium Duty/Heavy Duty Vehicle Project. The views expressed in the article do not necessarily represent the views of the DOE or the U.S. Government. The U.S. Government retains and the publisher, by accepting the article for publication, acknowledges that the U.S. Government retains a nonexclusive, paid-up, irrevocable, worldwide license to publish or reproduce the published form of this work, or allow others to do so, for U.S. Government purposes.

References

[1] "TransBorder Freight Data | Bureau of Transportation Statistics." https://www.bts.gov/transborder (accessed Jun. 21, 2020).

[2] H. Liimatainen, O. van Vliet, and D. Aplyn, "The potential of electric trucks – An international commodity-level analysis," *Appl. Energy*, vol. 236, pp. 804–814, Feb. 2019.

[3] H. Parastvand, V. Moghaddam, O. Bass, M. A. S. Masoum, A. Chapman, and S. Lachowicz, "A Graph Automorphic Approach for Placement and Sizing of Charging Stations in EV Network Considering Traffic," *IEEE Trans. Smart Grid*, pp. 1–1, 2020.

[4] N. Sathaye and S. Kelley, "An approach for the optimal planning of electric vehicle infrastructure for highway corridors," *Transp. Res. Part E Logist. Transp. Rev.*, vol. 59, pp. 15–33, Nov. 2013.

[5] T. K. Kristoffersen, K. Capion, and P. Meibom, "Optimal charging of electric drive vehicles in a market environment," *Appl. Energy*, vol. 88, no. 5, pp. 1940–1948, May 2011.

[6] J. C. Gomez and M. M. Morcos, "Impact of EV battery chargers on the power quality of distribution systems," *IEEE Trans. Power Deliv.*, vol. 18, no. 3, pp. 975–981, Jul. 2003.

[7] C. Jiang, R. Torquato, D. Salles, and W. Xu, "Method to Assess the Power-Quality Impact of Plug-in Electric Vehicles," *IEEE Trans. Power Deliv.*, vol. 29, no. 2, pp. 958–965, Apr. 2014.

[8] G. Razeghi, L. Zhang, T. Brown, and S. Samuelsen, "Impacts of plug-in hybrid electric vehicles on a residential transformer using stochastic and empirical analysis," *J. Power Sources*, vol. 252, pp. 277–285, Apr. 2014.

[9] W. Gan *et al.*, "Coordinated Planning of Transportation and Electric Power Networks with the Proliferation of Electric Vehicles," *IEEE Trans. Smart Grid*, pp. 1–1, 2020.

[10] A. Shukla, K. Verma, and R. Kumar, "Multi-objective synergistic planning of EV fast-charging stations in the distribution system coupled with the transportation network," *Transm. Distrib. IET Gener.*, vol. 13, no. 15, pp. 3421–3432, 2019.

[11] G. Boeing, "OSMnx: New methods for acquiring, constructing, analyzing, and visualizing complex street networks," *Comput. Environ. Urban Syst.*, vol. 65, pp. 126–139, Sep. 2017.

[12] "GeoPandas 0.8.0 — GeoPandas 0.8.0 documentation." https://geopandas.org/index.html (accessed Jun. 30, 2020).

[13] R. Philipsen, T. Schmidt, J. van Heek, and M. Ziefle, "Fast-charging station here, please! User criteria for electric vehicle fast-charging locations," *Transp. Res. Part F Traffic Psychol. Behav.*, vol. 40, pp. 119–129, Jul. 2016.

[14] A. Bernstein, C. Wang, E. Dall'Anese, J.-Y. Le Boudec, and C. Zhao, "Load Flow in Multiphase Distribution Networks: Existence, Uniqueness, Non-Singularity and Linear Models," IEEE Trans. Power Syst., vol. 33, no. 6, pp. 5832–5843, Nov. 2018.